Issues Surrounding the Development of Models for use in Predicting Gas Turbine Combustion

Nigel S. A. Smith

DSTO-TN-0256

Issues Surrounding the Development of Models for use in Predicting Gas Turbine Combustion

Nigel S. A. Smith

Airframes And Engines Division
Aeronautical and Maritime Research Laboratory

DSTO–TN–0256

ABSTRACT

A general description is provided of current model development associated with Task DST 98/091 *Modelling Airbreathing Combustion*. This note describes current and future work towards the completion of a fully implemented software suite for turbulent combustor applications. Particular attention is paid to the issues surrounding applying the Conditional Moment Closure (CMC) family of models, which were developed in simple flows, to flow cases of practical interest. These issues include the integration of radiation heat transfer, conductive heat transfer, complex recirculating flow, and complex chemistry within the CMC model context.

20010302 184

APPROVED FOR PUBLIC RELEASE

DSTO–TN–0256

APPROVED FOR PUBLIC RELEASE

Issues Surrounding the Development of Models for use in Predicting Gas Turbine Combustion

EXECUTIVE SUMMARY

The prediction of combustion within gas turbine engine combustors (GTCs) is a critical requirement for understanding how to successfully operate gas turbine engines and the platforms in which they are installed. The combustion processes which occur in GTCs govern important operational issues such as engine component lifetimes, engine performance, stability of engine operation, and detectable emissions. Thus the ability to comprehensively predict all aspects of gas turbine combustion can usefully aid in the diagnoses of poor engine performance and unusual component degradation, as well as provide inputs to the estimation of platform infra-red and visible signatures.

By developing a modelling philosophy based upon fundamental physical processes, rather than empirical observation of particular engines, an inherent flexibility is lent to the final model. This allows it be to applied across all existing engine types, and indeed, to predictions of the characteristics of foreign-operated and future engines. Task DST 98/091 *Modelling Airbreathing Combustion* was established to provide DSTO and the ADO with a fundamentally based GTC predictive capability, implemented as a suite of numerical software. After one year of development, it is appropriate to pause and delineate the way forward in the research program. The purpose of this technical note is to provide just such a technical delineation.

The key physical processes which contribute to modelling GTCs are outlined in this note. These processes are described to result from interactions between four key elements of the overall physical system. These key elements, turbulence, combustion, heat transfer, and multi-phase flow, are each relatively well understood in isolation. While a myriad of mature modelling methodologies are available for each element in isolation, the integration of different models from different development backgrounds takes some care. This note describes in detail, some of the issues surrounding the implementation of a number of disparate models in a coherent model framework capable of being applied to gas turbine combustion prediction.

Author

Nigel S. A. Smith
Airframes and Engines Division

Nigel Smith completed a Bachelor of Engineering with Honours (Mechanical) at the University of Western Australia in 1990. His honours dissertation was a study of flow modification in flat-plate turbulent boundary layers as a result of riblet surface modifications, using laser doppler velocimetry.

Between 1991 and 1994, he studied towards a Ph.D. at the University of Sydney, in the Department of Mechanical Engineering. His research dealt with the development and testing of the Conditional Moment Closure method for predicting turbulent combustion processes. Along the way, he was able to travel and work extensively at the Combustion Research Facility at Sandia National Laboratories in Livermore, California, as well as at Cambridge University and the NATO Advanced Study Institute Workshop in Les Houches, France.

Upon completion of his Ph.D. research and thesis in September of 1994, he took up a position as a postdoctoral fellow at the Center for Turbulence Research, a joint research facility operated by Stanford University and the NASA Ames Research Center. After two years of research into turbulent combustion using direct numerical simulation, he found his way back from Northern California to Melbourne, where he has taken up an RS position in the Airframes and Engines Division.

Nigel Smith's current research objective is to provide DSTO with a credible in-house capability for the prediction of turbulent combustion dynamics in a generic gas turbine combustor setting. The successful implementation of this capability will allow DSTO to better serve the future needs of its customer as they arise, rather than after the fact.

Contents

1 Introduction

The prediction of combustion within gas turbine engine combustors (GTCs) is a critical requirement for understanding how to successfully operate gas turbine engines and the platforms in which they are installed. The combustion processes which occur in GTCs govern important operational issues such as engine component lifetimes, engine performance, stability of engine operation, and detectable emissions. Thus the ability to comprehensively predict all aspects of gas turbine combustion can usefully aid in the diagnoses of poor engine performance and unusual component degradation, as well as provide inputs to the estimation of platform infra-red and visible signatures.

By developing a modelling philosophy based upon fundamental physical processes, rather than empirical observation of particular engines, an inherent flexibility is lent to the final model. This allows it be to applied across all existing engine types, and indeed, to predictions of the characteristics of foreign-operated and future engines.

Currently, DSTO has a Task in place to develop a software suite to numerically predict combustion characteristics within GTCs and other steady constant-pressure nonpremixed combustion devices. Task DST 98/091 *Modelling Airbreathing Combustion* is at the end of its first year of execution. This note is designed to broadly outline the theoretical and technical issues which surround the continuing effort to develop and implement GTC model software.

The GTCs currently employed in modern aeropropulsion applications employ a *nonpremixed* combustion configuration. In this configuration, liquid fuel is sprayed into a stabilised recirculating air flow. The liquid fuel evaporates, mixes with surrounding hot gases, and burns concurrently within the fuel-rich recirculation zone. This type of configuration is employed in preference to *premixed* fuel-air delivery due to its inherent stability of operation over a wide range of power settings. The combination of a low-speed recirculation zone and a localised abundance of fuel in the zone ensure the presence of a flame under these various operating conditions. Further air is added downstream of the recirculation zone to complete the combustion of fuel present in the product gas stream. Still further air is progressively added to cool the stream to a point where the gas temperature is low enough to avoid damage to downstream components in the turbine assembly.

The overall process of heat injection into the stream passing through the combustor involves many interacting physical processes. Intense turbulent mixing is required within the combustor to bring fuel-rich and fuel-lean pockets of gas together at a rapid rate. This allows combustion reactions to proceed and the rapid release of heat in a confined volume to take place. The overall chemical reaction which is taking place within the combustor is only a global representation of the multitude of elementary reactions going on between many thousands of intermediate chemical species. These reactions proceed at rates which are non-linearly dependent upon temperature and species concentrations, and are variously accelerated and impeded by the turbulent mixing processes which continously change the distributions of these quantities. To further complicate the picture, the hot combusting mixture is continuously exchanging heat with the surrounding combustor surfaces through radiative absorption. The formation of soot particles from fuel rich gases significantly enhances this process, and at the same time adds the complication of a reacting solid-phase to the problem to be modelled. Transfer of heat to liquid fuel droplets and their

evaporation adds another aspect to the overall process.

Though there are many different physical processes inherent in GTC combustion, this note is limited in scope to separate discussions of a selected number of the modelling methods which will be implemented in the near future.

2   Modelling Methods

Many different submodels are required to be integrated into a whole in order to provide a model framework which is applicable to all aspects of nonpremixed airbreathing combustion. In Figure 1, the key physical elements of this framework, and the causal relationships between these elements has been conceptualised according to the diagram shown.

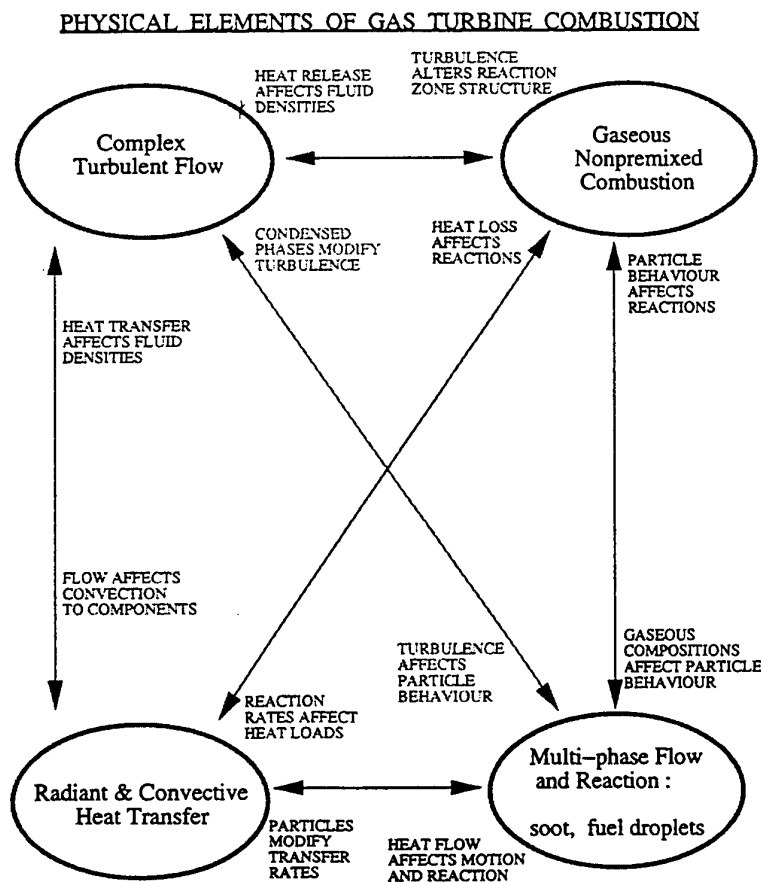## PHYSICAL ELEMENTS OF GAS TURBINE COMBUSTION

Figure 1: Schematic diagram indicating the interactions between key physical processes which require modelling in the context of a gas turbine combustor.

The model problem has been broken up into four key elements, namely turbulent flow and mixing in a complex geometry, gaseous nonpremixed combustion, heat transfer to boundaries, and multi-phase species dynamics. In Fig. 1, the processes governed by these key elements interact with one another to varying degrees. For example (see horizontal arrow at top of the figure), gaseous nonpremixed combustion is influenced by turbulent flow and mixing. The range of scales of turbulent motion cause pockets of reactive species to be mixed together at rates which can limit the overall rate of reaction and/or modify flame structures. Conversely, the heat release associated with combustion causes large spatial variations in fluid densities which then affect the momentum transfer characteristics within the flow field.

Another interaction is that where the heat release from gaseous combustion causes local temperature rises which lead to increased radiant and convective heat transfer. The presence of this heat transfer alters local temperatures which impacts upon the rates of chemical reactions in these regions.

The presence of condensed-phase particles, such as soot and fuel droplets, can cause gas phase reactions in their vicinity to be modified. In the case of soot, the solid phase particles are a source and sink of chemical species and enthalpy. In the case of fuel droplets, the liquid fuel is a sink for sensible enthalpy and a source of combustible fuel which evaporates off the droplet surface as a result of elevated temperatures in the adjacent gas.

The key to building the required model framework is in the selection of compatible submodels which have approximately the same degree of intrinsic accuracy in their selected application. The submodel with the poorest accuracy will adversely affect the overall predictive capability, and so it is important to avoid wasting effort in strengthening strong links in the chain while overlooking weaker links.

The traditionally weakest link in the model chain has been the modelling of the gaseous nonpremixed combustion element in the presence of turbulence. It is logical therefore to start the assembly of the model framework with the selection of an accurate turbulent combustion model. The bulk of this note is concerned with the practical details of this model.

2.1   Combustion modelling : CMC

When modelling turbulent nonpremixed combustion, difficulty is encountered in correctly determining mean chemical reaction rates. Unlike in chemically inert turbulent flow, simple Reynolds (or Favre) averaging of the flow field does not provide sufficient information to effect an adequate closure of the resultant averaged scalar equations. The highly non-linear dependence of chemical source terms on local temperature and reactant species concentrations, which fluctuate rapidly in turbulent flow, defeats any attempt at a linear first order closure in terms of the averaged local temperature and reactant concentrations. Many models for turbulent nonpremixed combustion have been devised over the past fifty years. One model is known as the Conditional Moment Closure (CMC) method [1, 2] and has been applied extensively to predicting species concentrations and temperatures in gas-fuelled turbulent jet flames [3]-[8]. Instead of employing conventional *unconditional* averaging of the instantaneous reactive species equations, the CMC method

involves solving conditionally averaged equations. The following provides a description of this method, its rationale, and applications.

The local instantaneous equation for the conservation of the mass fraction (Y_α) of a chemical species (α) can be written as,

$$\frac{\partial}{\partial t} (\rho Y_\alpha) + \frac{\partial}{\partial x_i} (\rho u_i Y_\alpha) - \frac{\partial}{\partial x_j} \left(\rho \mathcal{D}_\alpha \frac{\partial Y_\alpha}{\partial x_j} \right) = \rho \dot{w}_\alpha \tag{1}$$

where ρ is the fluid density, u_i is the i-th component of fluid velocity, $\mathcal{D}_\alpha$ is the molecular diffusivity (Fickian diffusion approximation) of the species α, and $\dot{w}_\alpha$ is the net chemical production rate of α.

Unconditional averaging of equation 1 results in,

$$\frac{\partial}{\partial t} (\langle \rho Y_\alpha \rangle) + \frac{\partial}{\partial x_i} (\langle \rho u_i Y_\alpha \rangle) - \frac{\partial}{\partial x_j} \left(\rho \mathcal{D}_\alpha \frac{\partial \langle Y_\alpha \rangle}{\partial x_j} \right) = \langle \rho \dot{w}_\alpha \rangle \tag{2}$$

with the resultant closure problem of the unconditional mean chemical source term,

$$\langle \rho \dot{w}_\alpha (Y_1, \ldots, Y_n, T) \rangle \neq \langle \rho \rangle \dot{w}_\alpha (\langle Y_1 \rangle, \ldots, \langle Y_n \rangle, \langle T \rangle) \ . \tag{3}$$

The above closure fails due to the size of instantaneous local deviations from the modelled unconditional mean values in the flow that is being modelled. The CMC model seeks to reduce the size of these deviations and thereby allow a similar first order closure (using different averaging operator) to succeed.

The CMC model seeks to employ an averaging process which accounts for turbulence-induced fluctuations. Mixture fraction (ξ) provides a useful measure of the degree of mixing between fuel and oxidizer masses, which is invariant under chemical reaction. Averaging based on conditions on the value of mixture fraction take account of turbulence-induced mixing fluctuations. Mixture fraction is a scalar which is derived from an appropriate linear combination of chemical scalars,

$$\xi \equiv \sum_{\alpha=1}^{N} a_\alpha Y_\alpha \tag{4}$$

such that the net chemical production of that scalar is identically zero,

$$\sum_{\alpha=1}^{n} a_\alpha \dot{w}_\alpha = 0 \ , \tag{5}$$

and is normalised so that (by convention) it has a value of unity in fluid that originated wholly from the fuel stream, and zero in fluid that originated in the oxidizer stream. It is necessary to refer to fuel and oxidizer 'origins' since while fuel and oxidizer may be chemically consumed in an isolated sample, the mixture fraction will remain unchanged. Thus the resultant mixture of products and remnant reactants will constitute the same value of mixture fraction as the original unreacted sample. Only the introduction of further mass (through mixing) to change the atomic population of the sample will have any bearing on mixture fraction. It is this invariance under reaction which makes mixture fraction such a useful *coordinate* in which to examine nonpremixed combustion.

The CMC method involves solving for the mean species mass fractions which result from conditionally averaging an ensemble of instantaneous local realisations of the turbulent flow in question. The conditional mean quantities are determined by discriminating between contributing samples on the basis of their associated value of mixture fraction. For a given conditioning value (η) of mixture fraction (ξ), only those samples simultaneously meeting the conditional criteria ($\xi(\underline{x},t) = \eta$) are allowed to contribute to the mean. Thus instead of traditional *unconditional* averaging, where averaging over an ensemble of points in time and space would only produce a single value, the conditional averaging process produces a profile of mean values,

$$Q_\alpha(\underline{x},t,\eta) \equiv \langle Y_\alpha(\underline{x},t) \mid \eta \rangle ,\qquad(6)$$

as a function of the conditioning variable abscissa (η).

Conditional averaging of the instantaneous local species mass fraction equations (eq 1) yields,

$$\langle \rho \mid \eta \rangle \frac{\partial Q_\alpha}{\partial t} + \langle \rho u_i \mid \eta \rangle \frac{\partial Q_\alpha}{\partial x_i} = N_\eta \frac{\partial^2 Q_\alpha}{\partial \eta^2} + \langle \rho \dot{w}_\alpha \mid \eta \rangle ,\qquad(7)$$

where N_η is the conditional mean scalar dissipation rate defined by,

$$N_\eta \equiv \left\langle \rho \mathcal{D}_\xi \left(\frac{\partial \xi}{\partial x_j} \right)^2 \mid \eta \right\rangle .\qquad(8)$$

The terms in equation 7, from right to left, account for solution unsteadiness, mean convective transport in physical space, turbulent mixing in mixture fraction space, and chemical reaction. Unlike in the case of unconditionally averaged equations, first order closure of the chemical reaction source term can usually be achieved by,

$$\langle \rho \dot{w}_\alpha (Y_1,\ldots,Y_n,T) \mid \eta \rangle \approx \langle \rho \mid \eta \rangle \dot{w}_\alpha (\langle Y_1 \mid \eta \rangle,\ldots,\langle Y_n \mid \eta \rangle, \langle T \mid \eta \rangle) ,\qquad(9)$$

owing to the smaller degree of individual sample deviations from the modelled mean quantities.

In practice the conditional mean scalar dissipation rate must be determined from the conservation equation for the mixture fraction probability density function (P_η),

$$\frac{\partial}{\partial t} (\langle \rho \mid \eta \rangle P_\eta) + \frac{\partial}{\partial x_i} (\langle \rho u_i \mid \eta \rangle P_\eta) = -\frac{\partial^2}{\partial \eta^2} (N_\eta P_\eta) .\qquad(10)$$

to ensure conservation of mass in physical space. This is typically done by using an assumed form of the probability density function (PDF) such as a beta function or clipped Gaussian distribution. Equations for unconditional mean mixture fraction and mixture fraction variance are solved in physical space and PDF evolution is thus determined by the evolution of these two controlling parameters. The evolution of the PDF then gives the correct form of the conditional mean scalar dissipation rate,

$$N_\eta = \frac{-1}{P_\eta} \int_0^\eta \int_0^{\eta'} \left[\frac{\partial}{\partial t} (\langle \rho \mid \eta \rangle P_\eta) + \frac{\partial}{\partial x_i} (\langle \rho u_i \mid \eta \rangle P_\eta) \right] d\eta'' d\eta' .\qquad(11)$$

It can be seen from equation 8 that N_η is a non-negative definite distribution in mixture fraction space. The boundary conditions upon equation 11 are well known [3, 9]. The

product $(N_\eta P_\eta)$ must have zero value and zero gradient at extreme values of mixture fraction.

Unconditional mean data can be recovered from conditional mean profiles through convolution with the appropriate mixture fraction PDF,

$$\langle Y_\alpha(\underline{x}, t) \rangle = \int_0^1 P_\eta(\underline{x}, t) \, \langle Y_\alpha(\underline{x}, t) \mid \eta \rangle \, d\eta \ . \tag{12}$$

2.1.1 Similarity zones in conditional statistics

Past applications of the CMC method have involved the use of assumptions of conditional statistical similarity in one or more physical directions to reduce the dimensionality of the problem being solved. Steady axisymmetric turbulent jet flames have been modelled by assuming that conditional statistics are invariant across the radius of the jet at any given axial location. This radial independence means that a single set of conditional mean profiles (one for each species) suffices to describe the behaviour at all radial points at a common axial location.

Further, due to the parabolic nature of the flow characteristics, it was possible to use simple marching schemes to advance the solutions from nozzle exit plane to end of the flame in each case. In effect, these simplifications allowed the whole steady-state reactive flow field to be computed progressively using a single cross-sectional set of conditional mean species profiles, which is marched along the jet axis subject to the CMC equations.

More generally, however, these types of assumptions on the dimensional degeneracy of the conditional statistics may not be applicable. In a worst case scenario, an individual conditional mean profile would have to be solved for each species at every grid location in physical space. Typically, between thirty and one hundred grid points are required in each mixture fraction profile to provide adequate resolution of nonpremixed flame structure. Thus in this worst case scenario, the CMC model may require up to two orders of magnitude more computer memory and very much more computation time than for the solution of a passive scalar.

For problems of practical interest, such as gas turbine combustors, it is important to take advantge of spatial similarities in conditional statistics as much as possible to minimise the number of independent profiles which must be carried by the model. It is useful to introduce the concept of conditional statistical *similarity zones*. A similarity zone is defined here as a region of space across which conditional statistics are spatially uniform to good approximation. Within a similarity zone, a single conditional mean profile for each species suffices to describe behaviour at all physical-space grid points.

In Figure 2, different notional boundaries for similarity zones are depicted for a variety of flow cases. On the left of the figure, the case for jet flames (described above) is depicted, with a radial marching similarity zone. In the centre of the figure, possible static similarity zones are depicted for an axisymmetric combustor can. The right hand side of Fig. 2 relates to the similarity zone approach used in the Conditional Source Evaluation (CSE) method [10], which is described in Section 2.1.3.

The *a priori* determination of static similarity zone boundaries in complex flow is arbitrary and somewhat problematic. In two dimensional calculations, streamlines may
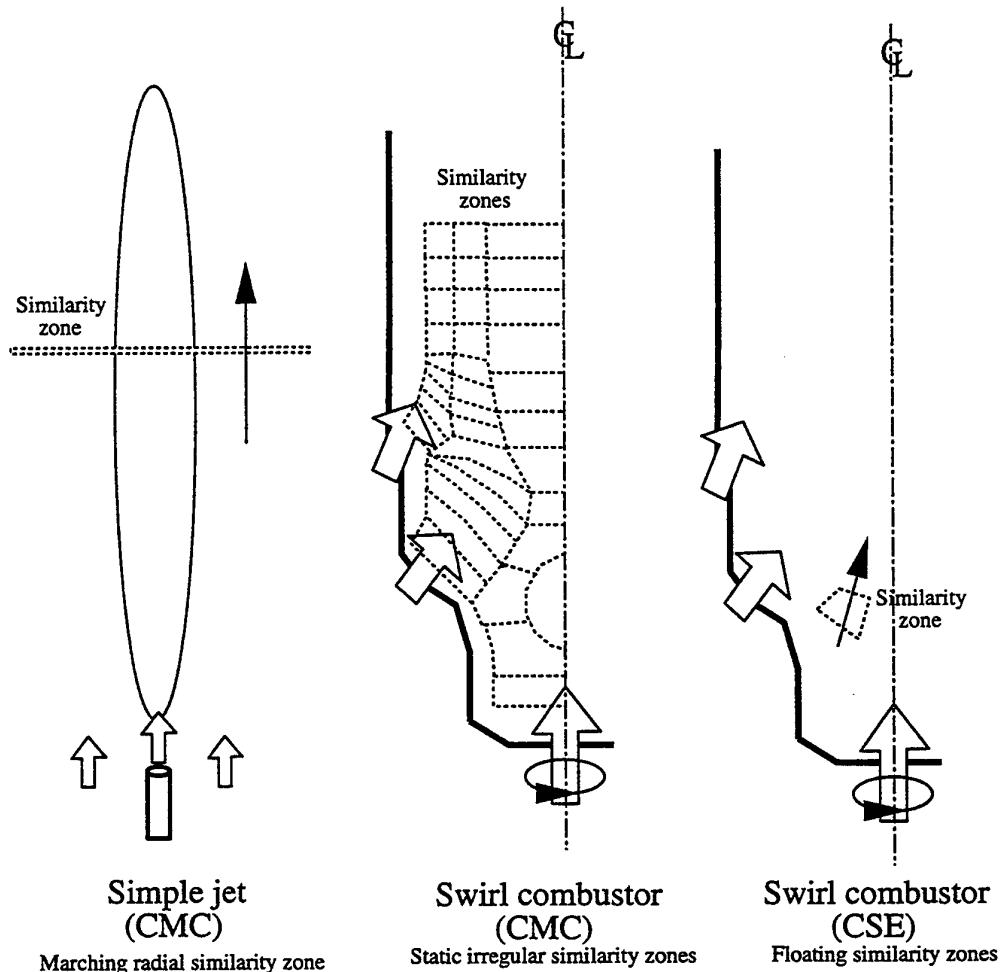
Figure 2: Schematic diagram indicating the differences in conditional statistical similarity zone structure in jet flames and swirl combustors for CMC and CSE methods.

be used as a guide in the apportioning of the domain into similarity zones. As with the simple jet flow, it is appropriate that where streamlines are close and parallel, a similarity zone can be delineated across these streamlines. Thus in a locally-free shear layer, zone boundaries will be perpendicular to groups of parallel streamlines. In order to capture conditional mean species development, zones should be established at relatively small intervals along streamlines. Near walls and other flow boundaries, additional similarity zones may be required to capture gradients in reactive species. The establishment of a static zonal structure will probably require detailed knowledge of the flow field beforehand, perhaps using a cold flow solution as a guide.

Given the definition of a similarity zone, it is possible to average a divergence form of the conditional mean species equation (eqn 7) over the volume (V_Ω) of such a zone so

that,

$$\left\{ \frac{\partial}{\partial x_i} \left(\langle \rho u_i \mid \eta \rangle P_\eta Q_\alpha \right) - Q_\alpha \frac{\partial}{\partial x_i} \left(\langle \rho u_i \mid \eta \rangle P_\eta \right) \right\}_\Omega = \left\{ N_\eta P_\eta \frac{\partial^2 Q_\alpha}{\partial \eta^2} + \langle \rho \dot{w}_\alpha \mid \eta \rangle P_\eta \right\}_\Omega ,$$

(13)

where $\{\ldots\}_\Omega$ denotes the volume averaging operator. It is possible to further simplify the above equation to eliminate one of the left hand side convective terms. However, in the light of the potentially irregular boundaries of similarity zones, the above divergence form is easier to accurately implement.

Application of Gauss's Theorem and the independence of conditional mean species data upon physical location give,

$$\langle F_Q \mid \eta \rangle - Q_\alpha \langle F_P \mid \eta \rangle = \{N_\eta\}_\Omega \frac{\partial^2 Q_\alpha}{\partial \eta^2} + \langle \rho \dot{w}_\alpha \mid \eta \rangle ,$$

(14)

where $\langle F_Q \mid \eta \rangle$ and $\langle F_P \mid \eta \rangle$ denote conditional mean species mass flux and conditional mean mass flux, across the zone-bounding surface. These fluxes are defined as,

$$\langle F_Q \mid \eta \rangle \equiv \frac{1}{\{P_\eta\}_\Omega V_\Omega} \oint_S \langle \rho u_i \mid \eta \rangle' P_\eta' Q_\alpha' ds_i$$

(15)

$$\langle F_P \mid \eta \rangle \equiv \frac{1}{\{P_\eta\}_\Omega V_\Omega} \oint_S \langle \rho u_i \mid \eta \rangle' P_\eta' ds_i ,$$

(16)

where V_Ω is the volume of the similarity zone. The conditional mean quantities at the bounding interface have intermediate values between those of the adjacent zone and the current zone. Intermediate valued quantities are indicated in the above definitions by superscript prime symbols. The companion mixture fraction PDF equation can be treated similarly to the CMC equation to yield,

$$\langle F_P \mid \eta \rangle \{P_\eta\}_\Omega = -\frac{\partial^2}{\partial \eta^2} \left(\{N_\eta P_\eta\}_\Omega \right) .$$

(17)

The similarity zone formulation embodied by equations 14-17 provides a means for employing the CMC method in cases of practical interest. Care must be taken in implementation of these equations to maintain their adjoint relationship. Failure to do so would result in a failure to conserve mass within the model.

2.1.2 Determining conditional mean auxilliary variables

Conditional mean quantities such as velocity ($\langle u_i \mid \eta \rangle$) and scalar dissipation rate (N_η) must be determined from unconditional mean data in order to solve equations 7-17. Within a conditional statistical *similarity zone* (see Section 2.1.1) these variables are related to the unconditional mean variables through convolution with the mixture fraction PDF,

$$\langle u(\underline{x}) \rangle = \int_0^1 \langle u \mid \eta \rangle P_\eta(\underline{x}) d\eta + e_u(\underline{x})$$

(18)

$$\langle N(\underline{x}) \rangle = \int_0^1 N_\eta P_\eta(\underline{x}) d\eta + e_N(\underline{x}) ,$$

(19)

where the PDF is itself usually an assumed-form distribution, dependent upon mixture fraction mean $\langle \xi \rangle (\underline{x})$ and variance $\langle \xi'^2(\underline{x}) \rangle$. It is appropriate to include the small error terms $e_u(\underline{x})$ and $e_N(\underline{x})$ in the above expressions to account for imperfect conditional statistical similarity within a designated zone. In order to determine the conditional mean data, a solution must be found for the above *Fredholm integral equations of the first kind* [11].

Where there are many grid points in a similarity zone with different unconditional mean values, it is possible to employ zeroth-order linear regularisation [11] to estimate the conditional mean data for the zone which correspond to these unconditional mean values. The basis for linear regularisation is perhaps better understood when a discretised form of the above equations is written as a linear problem,

$$\mathbf{A} \cdot \mathbf{u} + \mathbf{e} = \mathbf{b} \ , \tag{20}$$

where the matrix $\mathbf{A}$ represents the discretised form of the PDF convolution at a variety of points in physical space, $\mathbf{b}$ represents the unconditional mean values at points in physical space, $\mathbf{e}$ denotes the small errors at points in physical space due to imperfect conditional similarity, and $\mathbf{u}$ represents the conditional mean values in mixture fraction space. The matrix $\mathbf{A}$ is usually singular since the convolution is essentially a smoothing process and, further, their is no requirement for $\mathbf{A}$ to be square in any case. Thus the problem is likely to be ill-posed.

Linear regularisation involves forming a functional of $\mathbf{u}$, which is a global measure of the size of the unknown zonal similarity errors,

$$f_u = \mid \mathbf{A} \cdot \mathbf{u} - \mathbf{b} \mid^2 \tag{21}$$

and minimising the sum of this functional and an *a priori* functional,

$$g_u = \mid \mathbf{B} \cdot \mathbf{u} \mid^2 \tag{22}$$

which represents a global measure of the tendency for $\mathbf{u}$ to display a certain profile shape in mixture fraction space. The composition of the matrix $\mathbf{B}$ is selected according to the anticipated form of the conditional mean data, be it essentially constant, linear, parabolic, or any hybrid of these forms in mixture fraction space [11]. The addition of the *a priori* information places further constraints on the form of $\mathbf{u}$ so that the linear system is no longer singular and a unique solution is then possible for a given combination of the two functionals. The overall minimisation of $f_u + \gamma g_u$, subject to a threshold value of f_u, can be written as a normal linear equation of the form,

$$(\mathbf{A}^{\mathbf{T}} \cdot \mathbf{A} + \gamma \mathbf{B}^{\mathbf{T}} \cdot \mathbf{B}) \cdot \mathbf{u} = \mathbf{A}^{\mathbf{T}} \cdot \mathbf{b} \tag{23}$$

where γ is the blending factor with $0 < \gamma < \infty$ through which the minimisation is achieved.

It can be seen that very large γ values will cause minimisation to be based solely on $\mathbf{u}$ conforming to the *a priori* assumed shape, rather than matching the unconditional mean data. Conversely, very small γ values cause minimisation to be based solely on matching the unconditional mean data, which as stated above, will not have a unique solution if the number of points in mixture fraction space exceeds the number of physical grid points present in the zone. Where a unique solution does exist in cases of $\gamma \to 0$, it often exhibits

wild oscillations that, while satisfying the unconditional mean data set, are not physically plausible.

Press *et al* [11] suggest that the blending factor should be selected so that the lower threshold values of functional f_u should not be less than an estimate of the overall error associated with the $e_u(\underline{x})$ terms. To have an unreasonably lower threshold value invites unphysical profile behaviour as a result of too many degrees of freedom in the conditional mean profile. Estimates of the overall error which should be associated with e_u and e_N can be made based on the unconditional mean values for each variable and the coarseness of the similarity zones employed.

There are two alternate means by which the CMC and PDF equations (14, 17) can be solved using the auxilliary variables $\langle u_i \mid \eta \rangle$ and N_η. The first involves determining $\langle u_i \mid \eta \rangle$ from linear regularisation of the unconditional mean velocity fields ($\langle u_i \rangle$) within each similarity zone. The conditional mean velocity is then used in conjunction with equation 17 to find the conditional mean scalar dissipation rate $\{N_\eta\}_\Omega$). These two quantities are then used in the solution of equation 14. This procedure is preferrable since it retains the strong link between the two equations, required to conserve mass. This procedure can cause some difficulty in ensuring boundary conditions and realisability conditions are met for N_η. Smith [3] describes some of the difficulty which can arise from solving for N_η from the PDF equation directly. It was found that in many cases, inaccurate solutions for the $\langle \xi \rangle$ and $\langle \xi'^2 \rangle$ fields, which determine P_η and its spatial variation, can generate unrealisable N_η profiles which can quickly destabilise the CMC equations. These inaccurate solutions are likely in the early iterations of an iterative steady state solver, and some means must be available to otherwise approximate N_η under these circumstances.

The second means of determining N_η is far less prone to failing the realisability constraints. This procedure involves determining N_η by linear regularisation from the unconditional mean scalar dissipation rate $\langle N \rangle$ which is generated in the solution of the $\langle \xi'^2 \rangle$ equation. This second technique can provide provisional N_η profiles for use in the CMC equations where the first technique is yielding non-physical profiles due to poorly converged mixture fraction fields.

2.1.3 CSE method

The Conditional Source Evaluation (CSE) method was proposed by Bushe and Steiner [10] as a use of linear regularisation to predict chemical reaction rates in turbulent non-premixed combustion. The CSE method seeks to remedy the classical closure problem (see equation 3) directly without having to solve the CMC equations. Instead, chemical species transport and mixing is solved in terms of unconditional mean variables (as in equation 2). At each step where unconditional mean chemical reaction rates are required, conditional mean species profiles are determined from the unconditional mean species data using linear regularisation, and this conditional mean information is used to evaluate conditional mean reaction rates. These reaction rates are convolved with mixture fraction PDFs to return unconditional mean reaction rates.

The success or failure of the method depends to a very large extent on the accuracy of the linear regularisation which determines the conditional mean species profiles. As with the similarity zone formalism in CMC modelling, CSE also requires a similarity zone in

order to allow linear regularisation to take place. Static similarity zones (see Fig. 2) can be employed as in the CMC model with minimal computational effort. Alternatively the CSE method can employ a floating similarity zone for each physical grid point. Each of these similarity zones then includes the local grid points surrounding the point for which reaction rates are being determined.

The major problem with the CSE method is that the regularisation process can produce conditional mean species profiles which violate atomic mass balances, resulting in impossible chemical compositions. These compositions can destabilise the system of chemical reactions causing the computation to diverge.

A simple test can be derived to determine the accuracy of the CSE method. By taking known conditional mean chemical profiles (say resulting from a chemical equilibrium calculation), and convolving them with known PDFs, a set of unconditional mean data can be derived. The test for the CSE method is to return the conditional mean data from the unconditional mean data. Such a test was performed using species profiles corresponding to equilibrium conditions for C_2H_4 and air at a variety of equivalence ratios.
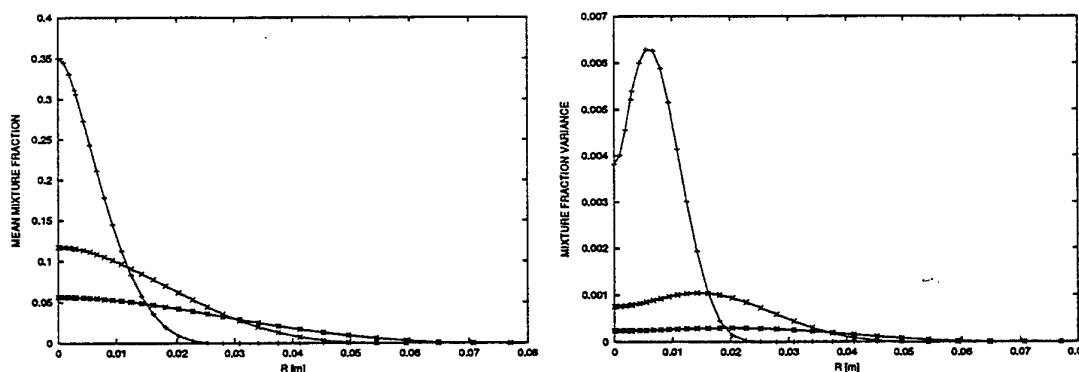

*Figure 3: Plots of mixture fraction unconditional mean and variance as functions of radial position at various axial locations in a 30 m/s C_2H_4 jet flame. Symbols denote axial location relative to the stoichiometric flamelength as : + - $x/L = 1/3$, × - $x/L = 2/3$, and * - $x/L = 1$*

The mixture fraction PDF values were determined to be beta functions depending upon the mean and variance of mixture fraction at a series of physical points taken from radial slices through an axisymmetric *fast chemistry* jet flame calculation. Figure 3 contains plots of the unconditional mean and variance of mixture fraction as functions of the radial location in each of these slices. It can be seen that the centreline mean mixture fraction decays with increasing axial distance from the nozzle, while the half-width of the jet spreads, as jet fluid is mixed with surrounding fluid. The mixture fraction variance peaks upstream near the interface between the pure fuel and pure oxidizer streams in the jet flow. The variance rapidly decays as a result of diffusive dissipation as the fluid moves downstream.

Using chemical equilibrium conditional mean profiles, and the mixture fraction PDFs resulting from the above mixture fraction distributions, unconditional mean species data was generated as input to the CSE integral equation solver. The *a priori* information
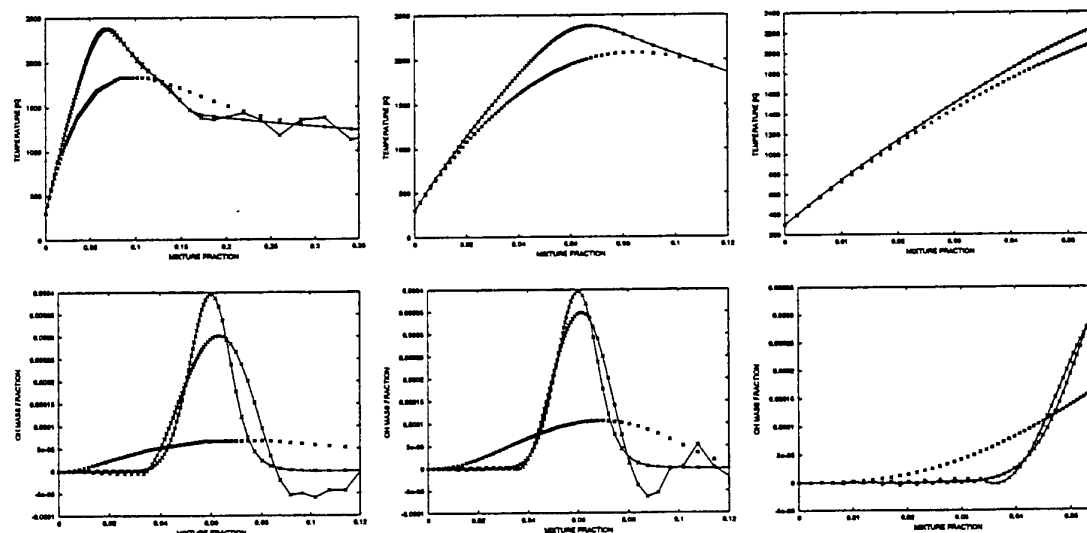
Figure 4: Temperature and OH radical mass fraction as functions of mixture fraction at various axial locations in a C_2H_4 jet flame. From the left to right, the plots correspond to $x/L = 1/3, 2/3, 1$. In each figure, the symbols denote, $\times$ a priori conditional mean data, $+$ CSE model estimate of a priori data, and $*$ unconditional mean species data determined from a priori data and used as input to CSE.

matrix **B** was carefully constructed for each species to select for the correct profile shape in mixture fraction space. For regions where the equilibrium conditional mean data was essentially constant, that portion of the **B** matrix was made to represent a first derivative operation. Regions of essentially linear behaviour were represented by a second derivative operator, and regions of parabolic behaviour were represented by a third derivative operator. Minimisation subject to **B** thus sought to minimise slope in regions thought to be constant, curvature in regions thought to be linear, and change in curvature in regions thought to be parabolic.

Figure 4 shows the results of the CSE integral equations compared with the *a priori* conditional mean profiles which they should match and the input unconditional mean profiles generated by the *a priori* conditional mean information. The two reactive scalars plotted are indicative of the type of agreement found for all of the chemical species employed. In each plot, the range in mixture fraction plotted corresponds with the range in mean mixture fraction found in the radial slice in question. As no unconditional data exists for mixture fractions outside this range it is not possible to accurately determine conditional mean profiles in these regions using linear regularisation.

It is apparent that the agreement between the imposed and modelled conditional mean temperature profiles is good at all axial locations but improves somewhat at greater distances from the nozzle. The agreement is poorer for the radical species OH, with the modelled profiles containing unphysical negative mass fractions at some mixture fractions. The agreement between the OH profiles does, however, improve at the downstream locations. The reason for the gradual improvement in agreement for all species with axial

distance from the nozzle, is that the mixture fraction variance decays so that unconditional mean values are more representative of conditional mean values. Integral equation solutions are most easily found when the unconditional mean data points are separated in mixture fraction space by many standard deviations of mixture fraction. Lower variances give rise to a smaller degree of overlap between the mixture fraction PDFs corresponding to different physical locations.

The unphysical appearance of negative mass fractions requires special handling before using the conditional mean species profiles to determine conditional mean reaction rates. Simple clipping of negative mass fractions to zero may be sufficient to avoid numerical instability. The results shown above indicate that the CSE method may be a useful alternative to the CMC model in the prediction of turbulent nonpremixed combustion.

2.2 Heat Transfer

To date, CMC modelling has been limited to applications of free-shear flows, such as turbulent jet flames. The absence of walls in these applications obviates the need for a means of treating conductive heat transfer to solid surfaces. However, practical application of CMC modelling demand a capability for dealing with heat transfer to adjacent walls.

In the immediate vicinity of a wall, some of the underpinning assumptions of the CMC method break down. The existence of a laminar sub-layer preclude the high Reynolds number turbulent transport approximations which permeate the model. Thus conditional similarity zones cannot be extended to walls. There must be an interface between the wall and the adjacent similarity zone boundary. Heat diffuses across this interface to the wall according to,

$$\langle \dot{s}^c \rangle \equiv \frac{\partial \langle q_i^c \rangle}{\partial x_i} \; , \tag{24}$$

where $\langle \dot{s}^c \rangle$ denotes the unconditional mean energy loss from the fluid due to conduction, and $\langle q_i^c \rangle$ denotes the unconditional mean heat flux in the i-th direction due to conduction. The heat flux is given by,

$$\langle q_i^c \rangle = -\lambda \frac{\partial \langle T \rangle}{\partial x_i} \; , \tag{25}$$

where λ is the thermal conductivity, a function of molecular activity, and $\langle T \rangle$ is the unconditional mean temperature.

Note that in the purely turbulent portion of the flow, heat conduction by molecular transfer is effectively incorporated into a turbulent thermal diffusivity term, which has a conditional mean counterpart in the CMC equations for standardised enthalpy. At the edge of turbulent region special boundary terms must be employed to account for this laminar heat transfer effect. It is proposed that a conditional mean conductive loss term $\{\langle \dot{s}^c \mid \eta \rangle\}_\Omega$ be employed in wall-boundary zones.

In cases with specified wall temperatures, the unconditional mean heat loss across the wall interface can be determined using unconditional mean temperatures at the zone boundary. These temperatures can be determined using the convolution,

$$\langle T(x) \rangle = \int_0^1 \{\langle T \mid \eta \rangle\}_\Omega P_\eta(x) d\eta \; . \tag{26}$$

The computed unconditional mean sources along the interface can then be employed to determine conditional mean sources using linear regularisation (see Section 2.1.2) of the following,

$$\langle \dot{s}^c(\underline{x}) \rangle = \int_0^1 \{ \langle \dot{s}^c \mid \eta \rangle \}_\Omega \, P_\eta(\underline{x}) d\eta \ . \tag{27}$$

In the case of wall boundaries where the heat flux is specified, the wall temperatures are inferred from the unconditional mean temperatures on the adjacent bound of the adjacent similarity zone. Regularised solutions for conditional mean heat flux are applied to the CMC equations as in the specified temperature boundary condition.

It is worth noting that it is also possible to use this procedure to account for unusual effects such as chemical species migrating to and from the wall as a result of molecular diffusion. Such an approach will be useful if surface chemistry (like platinum-film catalysis) is to be treated. Provided the overall mass balance between the wall and turbulent fluid is maintained this process will not influence the conserved scalar field upon which conditional averaging is predicated.

2.2.1 Radiation heat transfer

Radiation heat transfer has been modelled in the past using the assumption of an *optically thin* emitting media. Under this assumption, radiation emitted by hot gases is transmitted from the domain without any reabsorption or scattering whilst in transit. This assumption reduces radiant heat loss to being solely a function of local conditions rather than a non-local function of conditions throughout the domain.

The local nature of the optically thin radiation treatment allows a conditional mean heat loss term to be applied in the CMC equations without any need for describing geometric disposition of the domain. Thus

$$\langle \dot{s}^r \mid \eta \rangle \approx 4\pi\sigma \, k_p \left(\langle T \mid \eta \rangle, \langle Y_{H2O} \mid \eta \rangle, \langle Y_{CO2} \mid \eta \rangle, \langle Y_{SOOT} \mid \eta \rangle, \ldots \right) \langle T \mid \eta \rangle^4 \ , \tag{28}$$

applies where σ denotes the Stefan-Boltzmann constant, and k_p denotes the Planck mean absorption coefficient for the mixture at the given mixture fraction.

The optically thin assumption has been found to be a good approximation in many non-sooting combustion applications where physical dimensions are of a laboratory or aero-engine scale. The possibility exists, however, that the assumption will break down in the presence of soot and that parts of the domain may absorb energy transmitted from other parts of the domain. Under these circumstances, the geometric disposition of the participating media and the domain boundaries must be included in the calculation of radiant transfer.

A Finite Volume Radiation (FVR) model [12, 13] can be employed under these circumstances to predict radiation heat transfer. Flux intensities must be calculated for each incremental solid angle of direction for the boundaries of each grid cell. The balance of transmitted intensity into and out of each direction in each cell is made up by the net emission or absorption within that cell. The result is a large system of unconditional mean intensity equations which must be inverted at each step. Though tedious, this process is relatively straight-forward.
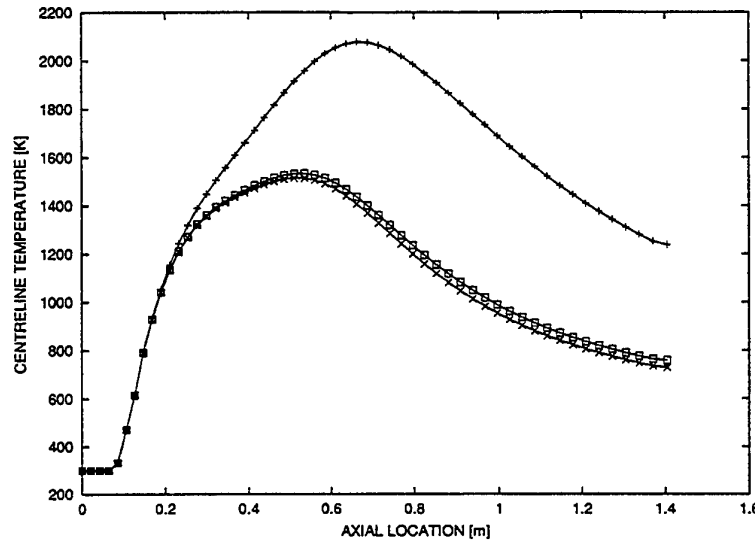
Figure 5: Comparison of unconditional mean centreline temperature variations with axial distance from the nozzle in a sooting C_2H_4 jet flame, for different radaition heat loss models. Symbols denote models according to :   + no model,   × optically-thin model, and □ FVR model.

Determination of the unconditional mean fourth-power of temperature is required in each grid cell in order to determine unconditional mean absorption and emission. This can be determined from the convolution of the conditional mean temperature, raised to the fourth-power, with the mixture fraction PDF in each grid cell. Conversely, the energy source/sink effect upon the CMC system of equations is that the unconditional mean emission or absorption in each grid cell must be regularised to generate conditional mean emission/absorption terms. The regularisation follows the same process as that described in the preceding sections.

While feasible, use of radiation models of the complexity of the FVR models, adds a large computational burden to the already expensive task of turbulent combustion modelling. It is worthwhile in most cases to determine ahead of time if use of these models is warranted over a vastly simpler optically-thin radiation model. This can be done using a simple fast chemistry or laminar flamelet model for turbulent combustion (see [7]). These models have poor predictive capability in most problems of interest, but are computationally cheap and will give good order-of-magnitude estimates for the purposes of determining if an FVR model is required for the treatment of radiation.

This type of analysis has been employed in the following example for a turbulent axisymmetric C_2H_4 sooting jet flame surrounded by adiabatic walls at a radial distance of 80 nozzle diameters. Laminar flamelet calculations were made where radiant heat loss to the walls was computed using optically-thin and FVR treatments. Figure 5 provides a comparison of the centreline unconditional mean temperature ($\langle T \rangle$) distributions in the flame which result from the application of the FVR model, the optically-thin model, and no model at all (no radiation heat loss). It is apparent that the difference between the

results predicted by the two radiation models is very slight in this case compared to the results for an adiabatic flame. The short path lengths for radiation emission through the flame in this computation, and the uniform bounding geometry make the optically-thin model a good choice for such a case.

2.3 Chemical Reactions

The presence of chemical reaction rates in the CMC equations (Eq 13), with timescales which vary by many orders of magnitude, cause these equations to be numerically *stiff*. Stiff equation sets are those where there is a wide disparity between the largest and smallest timescales associated with source terms. The scales of interest in most systems are those which change relatively slowly and iterative solution steps have a size in accordance with these timescales. Stiff systems of equations require the iterative step sizes to be commensurate with the shortest timescales, and yet the duration of the calculation must still run for a period in step with the longest scales.

Special solution algorithms must be employed to solve numerically stiff systems of equations which require a great deal more computational effort than the simple solvers which are employed for pure fluid dynamic problems. In practice, direct integration of these source terms typically requires $95 - 99\%$ of the overall CPU time devoted to an entire computation including Favre-averaged turbulence modelling, and the other terms in the CMC equations. Stiffness can be largely avoided in cases which employ reduced chemical reaction mechanisms. Those reduced schemes which eliminate the computation of key radical species such as H, OH and OH also eliminate the fastest reactions which are the cause of worst of the stiffness. However, in eliminating these species from direct computation, their important influence in determining many combustion characteristics is lost from the model.

Another means of decreasing the amount of CPU time spent in integrating chemical source terms involves *in situ* adaptive tabulation (ISAT). The results of integration of chemical terms are stored in a dynamic tree structure as the computation proceeds. Each integration is stored according to its start-point chemical composition and incremental time interval of integration. Computations are only made if a search of the tree structure reveals that a similar computation has not been already made. If a similar computation has been made, then the end-point chemical compositions of that computation are re-used. The definition of similar can be taken to mean that the search composition is within a short range of a stored start-point composition; short enough so that the results of integration of the search composition would result in end-point composition within a small distance from the stored end-point conditions.

A tree structure is used for data storage instead of an indexed table due to the excessive dimensionality that the latter would entail. An indexed table requires a separate array dimension for each chemical species as well as enthalpy and the interval of integration. Owing to the nature of the chemical reactions and the proliferation of unrealisable chemical states, the hyperspace described by such a table would be mostly empty and thus storage efficiency would be low.

The tree structure instead uses characteristic chemical species, enthalpy and time interval values to establish a test function as the sum of normalised entries in the composition
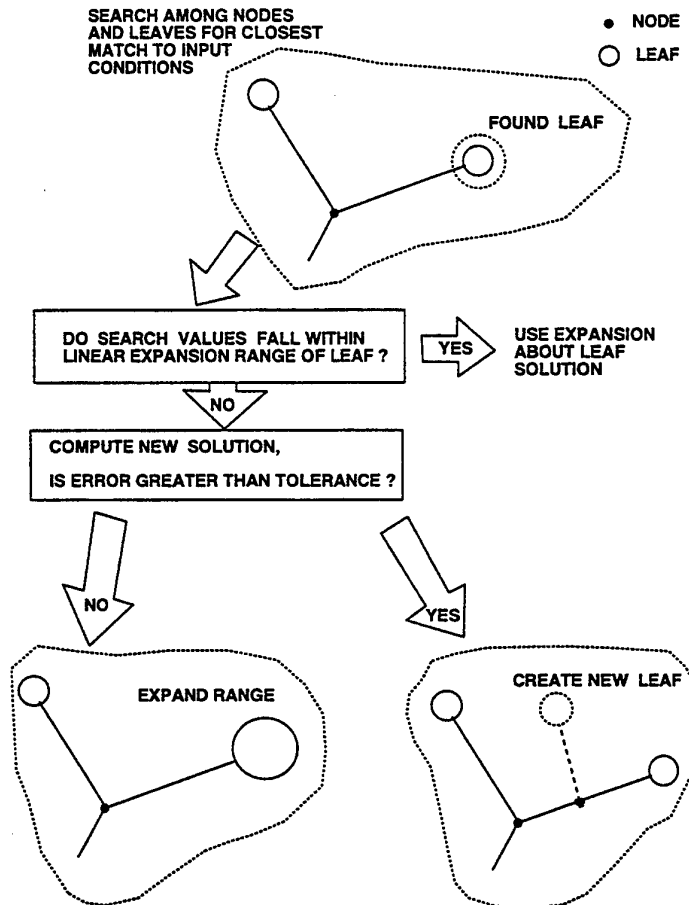
Figure 6: Graphic representation of the leaf and node creation algorithm employed in the in situ *adaptive tabulation scheme.*

/ enthalpy / time vector. The searching process proceeds by computing the value of this test function for the search composition. This value is then compared to values at tree nodes to the 'left' and 'right' of the current search node. A node is a storage location where values of the test function at nodes or leaves to the 'left' and 'right' are stored. The next search node becomes that to which the search value is closest. The difference between the new 'left' and 'right' nodes to the new search node is then smaller than the preceding difference, and so the search closes in on the closest stored composition to the search composition. Eventually the search reaches a stage where 'leaves' (accessible stored data) branch from nodes and one of these leaves is selected as the closest data to the search data.

The treatment of leaf data upon finding a matching leaf is illustrated by the diagram in Figure 6. Once a leaf has been found, the size of the discrepancy between the search composition and stored composition is determined. If this discrepancy is within a small range, then the stored end-point conditions are used as the integrated solution. If the

discrepancy is too large, then integration of the search composition is undertaken. If the end-point composition from this integration is dissimilar from the end-point composition of the leaf data, then a new leaf is established to save the newly-integrated result. In so doing, a new node is established between the old node and old leaf, and connectivity is reorganised so that the old node links to the new node instead of the old leaf, and the new node links to the old leaf and the new leaf. If the found-leaf's end-point composition is similar to the computed end-point composition, then no new leaf is generated and instead the leaf's start-point range is expanded to include the start-point search composition. In this instance the existing tree connectivity is retained.

The size of the end-point composition error tolerance is a determining factor in the number of leaves which will be generated in a given computation. If this error tolerance is large, then less leaves will be generated since it will be more probable that search compositions will fall within existing leaf ranges. Thus the overall computation will proceed faster since less integration is required, but at the expense of somewhat lower accuracy. Naturally, the reverse is true in that narrower error tolerances will tend to admit smaller errors, but cause more leaves to be generated and thus more integration steps to be taken.

The amount of computer memory available limits the size to which the tree can be allowed to grow. By recording the number of times individual leaves have been accessed and individual nodes have been traversed, it is possible to determine which parts of the tree are little used. These branches can be pruned as memory limits are reached to make way for new data produced by current calculations.

Trees generated from prior computations with similar chemistry can be used in new computations instead of growing trees from scratch. The amount of time saved in using an existing tree can be substantial. If, for example, a computation is repeated with the same chemistry on a slightly different grid, then one might reasonably expect that very few new chemical integrations will be required. In this case, computation time may be reduced by orders of magnitude.

For nonpremixed combustion it has been found that it is prudent to employ a number of trees, each storing data for chemical reactions occurring at widely different stoichiometries. This is done because of the very different nature of fuel-rich reactions and fuel-lean reactions for many fuels. To store the entire range of stoichiometries in a single tree can result in unnecessarily long search times. Trees can be indexed according to mixture fraction ranges, and tree searching can proceed within those broad ranges.

Past CMC computations of turbulent jet flames using ISAT for reaction mechanisms with 32 species and 111 reactions, have shown up to a $\sim 25\%$ saving in computation time. It should be pointed out however that these types of computations use a parabolic marching similarity zone to determine a steady state solution (see Section 2.1.1). This marching procedure does not call for repeated iterations of the same flow field and is thus not likely to derive much benefit from ISAT. It is expected that elliptic calculations of the type required in gas turbine combustor computations are likely to be accelerated by ISAT to a substantially greater degree.

3   Concluding Remarks

The key physical processes which contribute to modelling gas turbine combustors (GTCs) have been outlined. Taking a combustion model as a starting point, it has been described how the effects of turbulent mixing and heat transfer can be included.

The Conditional Moment Closure (CMC) model for turbulent nonpremixed combustion has been generalised to allow for its application in a GTC configuration, where complex recirculating flow, high turbulence levels, and significant heat transfer to bounding walls are all important. Perhaps the key aspect of this generalisation is the concept of *conditional similarity zones* which allow auxilliary conditional mean quantities to be computed from conventionally averaged quantities, using linear regularisation of the associated sets of integral equations.

A possible simpler alternative to the CMC model, the Conditional Source Evaluation (CSE) method has been described and evaluated. The CSE method makes extensive use of linear regularisation to solve for conditional mean chemical species profiles directly. The method shows some promise but requires further evaluation.

Finally, it was recognised that the numerical stiffness of the CMC equations can be significant and that repeated direct itegration of such stiff equations for very similar chemical steps is wasteful of resources. An adaptive tabulation method has been described to reduce the cost of solving chemical reaction steps in time, by storing and retrieving computed steps in a dynamic tree-storage structure.

Other aspects of GTC modelling, such as liquid fuel and other multi-phase effects, are also under current development [14, 15]. Those aspects, which have been omitted from discussion here, will also be implemented along with the models discussed in this note, in the remainder of Task DST 98/091.

References

1. Klimenko A. Yu.. 1990. "Multicomponent Diffusion of Various Admixtures in Turbulent Flow". *Fluid Dynamics*, v25, pp327-334.

2. Bilger R. W.. 1993. "Conditional Moment Methods for Turbulent Reacting Flow". *Physics of Fluids A*, v5, pp436-444.

3. Smith N. S. A., 1994. *Development of the Conditional Moment Closure Method for Modelling Turbulent Combustion*. PhD Thesis, University of Sydney.

4. Smith N. S. A., Bilger R. W., Chen J.-Y.. 1992. "Modelling of Nonpremixed Hydrogen Jet Flames using a Conditional Moment Closure Method". *Twenty-Fourth Symposium (International) on Combustion*, The Combustion Institute. pp263-269.

5. Smith N. S. A., Bilger R. W., Carter C. D., Barlow R. S., Chen J.-Y.. 1995. "A Comparison of CMC and PDF Modelling Predictions with Experimental Nitric Oxide LIF/Raman Measurements in a Turbulent H2 Jet Flame". *Combustion Science and Technology*, v105, p357.

6. Barlow R. S., Smith N. S. A., Chen J.-Y., Bilger R. W.. 1999. "Nitric Oxide Formation in Dilute Hydrogen Jet Flames: Isolation of the Effects of Radiation and Turbulence-Chemistry Submodels". *Combustion and Flame*, v117, pp4-31.

7. Smith N. S. A., 1998. *Comparison of CMC and SLF model predictions with experimental data for turbulent hydrogen jet flames*. DSTO Technical Report, DSTO-TR-0631, Aeronautical and Maritime Research Laboratory.

8. Smith N. S. A., 1998. *Comparison of soot model predictions with experimental data for a turbulent sooting propane jet flame*. DSTO Technical Report, DSTO-TR-0676, Aeronautical and Maritime Research Laboratory.

9. Klimenko A. Yu., Bilger R. W.. 1998. "Conditional Moment Closure for Turbulent Combustion". submitted to *Progress in Energy and Combustion Science*.

10. Bushe W. K., Steiner H.. 1998. "Conditional Source-term Evaluation for Large Eddy Simulation of non-premixed turbulent reacting flows". Private communication.

11. Press W. H., Flannery B. P., Teukolsky S. A., Vetterling W. T.. 1993. *Numerical Recipes : The Art of Scientific Computing*, Cambridge University Press.

12. Raithby G. D., Chui E. H.. 1990. "A Finite-Volume Method for Predicting a Radiant Heat Transfer in Enclosures with Participating Media". *Journal of Heat Transfer*, v112, pp415-423.

13. Chui E. H., Raithby G. D.. 1993. "Computation of Radiant Heat Transfer on a Nonorthogonal Mesh Using the Finite-Volume Method". *Numerical Heat Transfer*, v23, pp269-288.

14. Smith N. S. A., 1998. *Simulation and Modelling of Reacting Particles Relevant to Gas Turbine Combustion*. DSTO Research Report, DSTO-RR-0142, Aeronautical and Maritime Research Laboratory.

15. Smith N. S. A., Ruetsch G. R., Oefelein J., & Ferziger J., 1999. "Simulation and modelling of reacting particles in turbulent nonpremixed combustion", *Proceedings of the 1998 Summer Program*, Center for Turbulence Research, NASA Ames Research Center / Stanford University.

DISTRIBUTION LIST

Issues Surrounding the Development of Models for use in Predicting Gas Turbine
Combustion

Nigel S. A. Smith

Number of Copies

DEFENCE ORGANISATION

S&T Program

Chief Defence Scientist	
FAS Science Policy	1
AS Science Corporate Management	
Director General Science Policy Development	1
Counsellor, Defence Science, London	Doc Data Sht
Counsellor, Defence Science, Washington	Doc Data Sht
Scientific Adviser to MRDC, Thailand	Doc Data Sht
Scientific Adviser Policy and Command	1
Navy Scientific Adviser	Doc Data Sht
Scientific Adviser, Army	Doc Data Sht
Air Force Scientific Adviser	1
Director Trials	1

Aeronautical and Maritime Research Laboratory

Director, Aeronautical and Maritime Research Laboratory	1

Electronics and Surveillance Research Laboratory

Director, Electronics and Surveillance Research Laboratory	Doc Data Sht
Chief, AED	1
Research Leader, Propulsion, AED	1
Dr Simon Henbest, Head, Aerothermodynamics	1
Dr Nigel Smith, Task Manager	1

DSTO Research Library and Archives

Library Fishermans Bend	1
Library Maribyrnong	1
Library Salisbury	2
Australian Archives	1
Library, MOD, Pyrmont	Doc Data Sht
Library, MOD, HMAS Stirling	1
US Defense Technical Information Center	2
UK Defence Research Information Centre	2

Canada Defence Scientific Information Service	1
NZ Defence Information Centre	1
National Library of Australia	1

Capability Systems Staff

Director General Maritime Development	Doc Data Sht
Director General Land Development	1
Director General C3I Development	Doc Data Sht
Director General Aerospace Development	Doc Data Sht

Navy

SO(Science), Director of Naval Warfare, Maritime Headquarters Annex, Garden Island	Doc Data Sht

Army

ABCA Standardisation Officer, Puckapunyal	4
SO(Science), DJFHQ(L), MILPO, Enoggera, Queensland 4057	Doc Data Sht

Air Force

Intelligence Program

DGSTA, Defence Intelligence Organisation	1
Manager, Information Centre, Defence Intelligence Organisation	1

Acquisitions Program

Corporate Support Program

Officer in Charge, TRS, Defence Regional Library, Canberra	1

UNIVERSITIES AND COLLEGES

Australian Defence Force Academy Library	1
Head of Aerospace and Mechanical Engineering, ADFA	1
Deakin University Library, Serials Section (M List)	1
Hargrave Library, Monash University	Doc Data Sht
Librarian, Flinders University	1

OTHER ORGANISATIONS

NASA (Canberra)	1
Info Australia	1
State Library of South Australia	1
Parliamentary Library of South Australia	1

ABSTRACTING AND INFORMATION ORGANISATIONS

Library, Chemical Abstracts Reference Service	1

Engineering Societies Library, US	1
Materials Information, Cambridge Scientific Abstracts, US	1
Documents Librarian, The Center for Research Libraries, US	1

INFORMATION EXCHANGE AGREEMENT PARTNERS

Acquisitions Unit, Science Reference and Information Service, UK	1
Library – Exchange Desk, National Institute of Standards and Technology, US	1
National Aerospace Laboratory, Japan	1
National Aerospace Laboratory, Netherlands	1

SPARES

DSTO Salisbury Research Library	5

Total number of copies:	**52**

DEFENCE SCIENCE AND TECHNOLOGY ORGANISATION DOCUMENT CONTROL DATA	1. CAVEAT/PRIVACY MARKING

2. TITLE	3. SECURITY CLASSIFICATION
Issues Surrounding the Development of Models for use in Predicting Gas Turbine Combustion	Document (U) Title (U) Abstract (U)

4. AUTHOR	5. CORPORATE AUTHOR
Nigel S. A. Smith	Aeronautical and Maritime Research Laboratory 506 Lorimer St, Fishermans Bend, Victoria, Australia 3207

6a. DSTO NUMBER DSTO–TN–0256	6b. AR NUMBER AR–011–230	6c. TYPE OF REPORT Technical Note	7. DOCUMENT DATE March 2000

8. FILE NUMBER M1/9/655	9. TASK NUMBER DST 98/091	10. SPONSOR DSTO	11. No OF PAGES 21	12. No OF REFS 15

13. URL OF ELECTRONIC VERSION http://www.dsto.defence.gov.au/corporate/ reports/DSTO–TN–0256.pdf	14. RELEASE AUTHORITY Chief, Airframes And Engines Division

15. SECONDARY RELEASE STATEMENT OF THIS DOCUMENT

Approved For Public Release

OVERSEAS ENQUIRIES OUTSIDE STATED LIMITATIONS SHOULD BE REFERRED THROUGH DOCUMENT EXCHANGE, PO BOX 1500, SALISBURY, SOUTH AUSTRALIA 5108

16. DELIBERATE ANNOUNCEMENT

No Limitations

17. CITATION IN OTHER DOCUMENTS

No Limitations

18. DEFTEST DESCRIPTORS

Modelling	Heat Transfer
Combustion	Gas turbines
Computer Programs	Airbreathing engines

19. ABSTRACT

A general description is provided of current model development associated with Task DST 98/091 *Modelling Airbreathing Combustion*. This note describes current and future work towards the completion of a fully implemented software suite for turbulent combustor applications. Particular attention is paid to the issues surrounding applying the Conditional Moment Closure (CMC) family of models, which were developed in simple flows, to flow cases of practical interest. These issues include the integration of radiation heat transfer, conductive heat transfer, complex recirculating flow, and complex chemistry within the CMC model context.